Liquid transport generated by a flashing field-induced wettability ratchet

Karin John*

Laboratoire de Spectrométrie Physique,

Université Joseph Fourier - Grenoble I,

BP 87 - 38402 Saint-Martin-d'Hères, France

Uwe Thiele†

Max-Planck-Institut für Physik komplexer Systeme,

Nöthnitzer Str. 38, D-01187 Dresden, Germany

Abstract

We develop and analyze a model for ratchet-driven macroscopic transport of a continuous phase. The transport relies on a field-induced dewetting-spreading cycle of a liquid film with a free surface based on a switchable, spatially asymmetric, periodic interaction of the liquid-gas interface and the substrate. The concept is exemplified using an evolution equation for a dielectric liquid film under an inhomogeneous voltage. We analyse the influence of the various phases of the ratchet cycle on the transport properties. Conditions for maximal transport and the efficiency of transport under load are discussed.

PACS numbers: 68.15.+e, 47.20.Ma, 05.60.-k, 68.08.Bc

*Electronic address: kjohn@spectro.ujf-grenoble.fr

†Electronic address: thiele@mpipks-dresden.mpg.de; URL: http://www.uwethiele.de

Brownian ratchets present a well established way to induce directed motion of particles in spatially extended systems without global gradients, i.e. without a globally broken spatial symmetry [1, 2, 3]. Examples include colloidal particles suspended in solution that move when exposed to a sawtooth dielectric potential [4] and the selective particle filter formed by a micro-fabricated silicon membrane with asymmetrical bottleneck-like pores under application of an oscillating pressure gradient [5]. Brownian ratchets are also thought to represent the underlying mechanism of molecular motors that are responsible for the active transport of molecules along filaments in biological cells [6]. Brownian transport is based on a principle first pointed out by Pierre Curie [7] stating that also a macroscopically symmetric constellation may induce macroscopic transport if it exhibits local asymmetries, e.g. a periodic asymmetric potential that varies on a small length scale. However, the system has to be kept out of equilibrium, for instance, by a chemical reaction [6], an oscillating pressure [5] or electric potential [4].

Ratchets are not only used to transport or filter discrete objects like colloidal particles or macromolecules. A ratchet geometry may also serve to induce a macroscopic transport of a continuous phase using local gradients only. Experimentally investigated examples include a secondary liquid flow triggered in Marangoni-Bénard convection involving a solid substrate with asymmetric grooves [8]. On a similar substrate Leidenfrost drops perform a directed motion [9, 10]. Microdrops confined in asymmetrically structured geometries move when vibrating the substrate or applying an on/off electric field [11].

In this Letter we propose and analyse a simple generic model for ratchet driven free-surface flows resulting in the macroscopic transport of a continuous phase. The driving flashing ratchet is based on a switchable spatially periodic but asymmetric interaction of the liquid-gas interface and the solid substrate like, for instance, a field-induced wettability. One can envision several ways to experimentally realise the spatially inhomogeneous interaction and the switching in time. A simple setup consists of a thin film of dielectric liquid in a capacitor producing a sawtooth voltage profile when switched on. The electro-dewetting provoked by the application of a homogeneous electrical field is already used to structure thin films of liquid polymers [12, 13, 14].

An idealized electrical wettability ratchet (sketched in Fig. 1) works as follows. We consider a flat wetting film stable in the absence of an electric field (Fig. 1 (a)). Upon switching on an electric field at $t = 0$ (Fig. 1 (e)) the film is destabilized by both, the overall electric field and its local gradients (Fig. 1 (d)). This behavior is similar to dewetting on a heterogeneous substrate [15, 16]. After a transient it results in the collection of all the liquid in drops situated at the patches

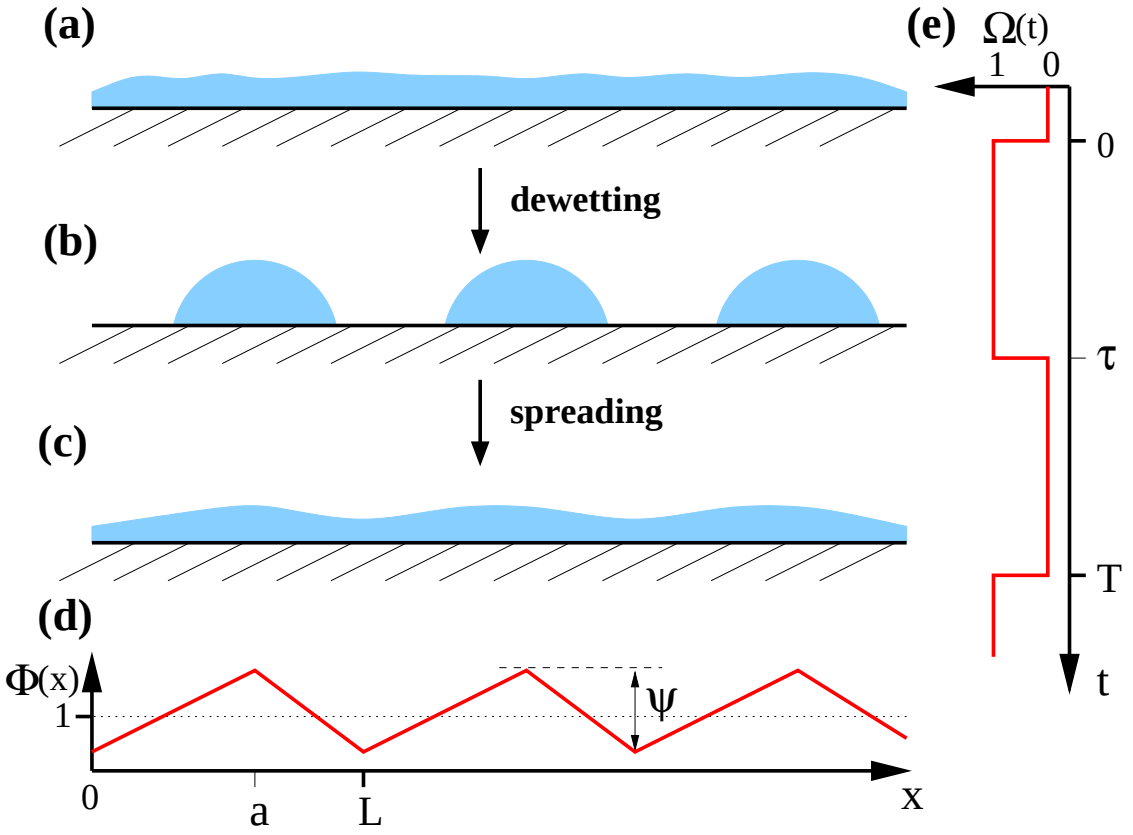

FIG. 1: Panels (a) to (c) illustrate the working principle of a fluidic ratchet based on a switchable wettability that causes dewetting-spreading cycles. (d) illustrates the spatial asymmetric periodic voltage profile $\Phi(x)$ responsible for the wettability pattern and (e) indicates the time dependence $\Omega(t)$ of the switching in relation to the dewetting and spreading phases in (a) to (c).

of maximal voltage (Fig. 1 (b)). After switching off the field at $t = \tau$ (Fig. 1 (e)) the drops spread into a homogeneous wetting layer (Fig. 1 (c)). Finally, at $t = T$ the field is switched on again and a new cycle starts. A typical realistic film dynamics during one ratchet cycle is shown in Fig. 2. For the geometry in Fig. 1 (d), with a voltage profile shaped like a sawtooth skewed to the right, each cycle transports liquid to the right.

The inhomogeneous electric field represents one out of several possible choices for a switchable spatially asymmetric interaction of liquid-gas interface and substrate. Others not pursued here include switchable brushes [17], heating [18, 19] or the switching of optical substrate properties, i.e. van der Waals interactions. Note however, that although length and time scales and the specific form of the resulting interaction potentials will differ, in principle all these realizations can be mapped onto our model using appropriate pressure terms corresponding to an effective switchable

'wettability'.

In presenting the dynamical model we restrict our attention to a two-dimensional system corresponding to a shallow open channel geometry and neglect the influence of the channel walls. The interplay of field-driven dewetting, liquid motion caused by local lateral gradients and spreading for small scale systems, i.e. of wettability and capillarity dominated fluid flow, is well described using an evolution equation for the film thickness profile [20]. A derivation from the basic transport equations using lubrication approximation gives

$$\partial_t\, h \;=\; \partial_x \left[\frac{h^3}{3\eta}\left(\partial_x\, p - f_{\rm ext}\right)\right] \tag{1}$$

where γ and η are the surface tension and dynamic viscosity of the liquid, respectively. $f_{\rm ext}$ denotes an external force in the direction of the x-axis. The change in time of the film thickness profile is given by the divergence of the flow, expressed as the product of a mobility and a pressure gradient and/or external force. The velocity field within the film is fully determined by the film thickness profile. The velocity parallel to the substrate is $u(x,z) \;=\; (z^2/2 - zh)\;\partial_x p$ and the vertical component is obtained using continuity. The pressure

$$p \;=\; -\,\gamma \partial_{xx} h \;-\; \Pi(h,x,t) \tag{2}$$

contains the curvature pressure $-\gamma\partial_{xx}h$ and the disjoining pressure $\Pi(h,x,t)$. The latter comprises the effective interactions between the liquid-gas interface and the substrate, i.e. the wettability properties [20, 21, 22]. Note, that the lubrication approximation can be formally applied to systems involving small surface slopes only. However, even for partially wetting systems with large contact angles, the lubrication approximation predicts in most cases the correct qualitative behavior [20].

As model system we use a dielectric oil in a capacitor of gap width d. The oil wets the lower plate and does not wet the upper plate corresponding to the van der Waals disjoining pressure

$$\Pi_{vdW} = \frac{1}{6\pi}\left(\frac{A_l}{h^3} + \frac{A_u}{(d-h)^3}\right) \tag{3}$$

with the Hamaker constants $A_l > 0$ and $A_u < 0$. A dielectric film in a capacitor with an applied voltage U_0 is subject to an electrical 'disjoining' pressure [12, 23]

$$\Pi_{el} = \frac{1}{2}\varepsilon_0\varepsilon_1 U_0^2\,\frac{(\varepsilon-1)}{[\varepsilon d + (1-\varepsilon)h]^2}. \tag{4}$$

where ε_0 and ε_1 are the absolute and relative dielectric constant, respectively and $\varepsilon \;=\; \varepsilon_1/\varepsilon_2$ denotes the ratio of the relative dielectric constants of the liquid and the gas phase. The modulation

of the electric field is periodic in x, but breaks parity, i.e. there exists no reflection symmetry in x. This ratchet potential is periodically switched on and off. In consequence Π in (2) takes the form

$$\Pi(h, x, t) = \Omega(t)\, \Phi(x)\, \Pi_{el}(h) + \Pi_{vdW}(h). \tag{5}$$

where the temporal variation $\Omega(t)$ and spatial variation $\Phi(x)$ are defined in Fig. 1 (a) and 1 (b), respectively, with $(1/L) \int_0^L \Phi(x)\, dx = 1$.

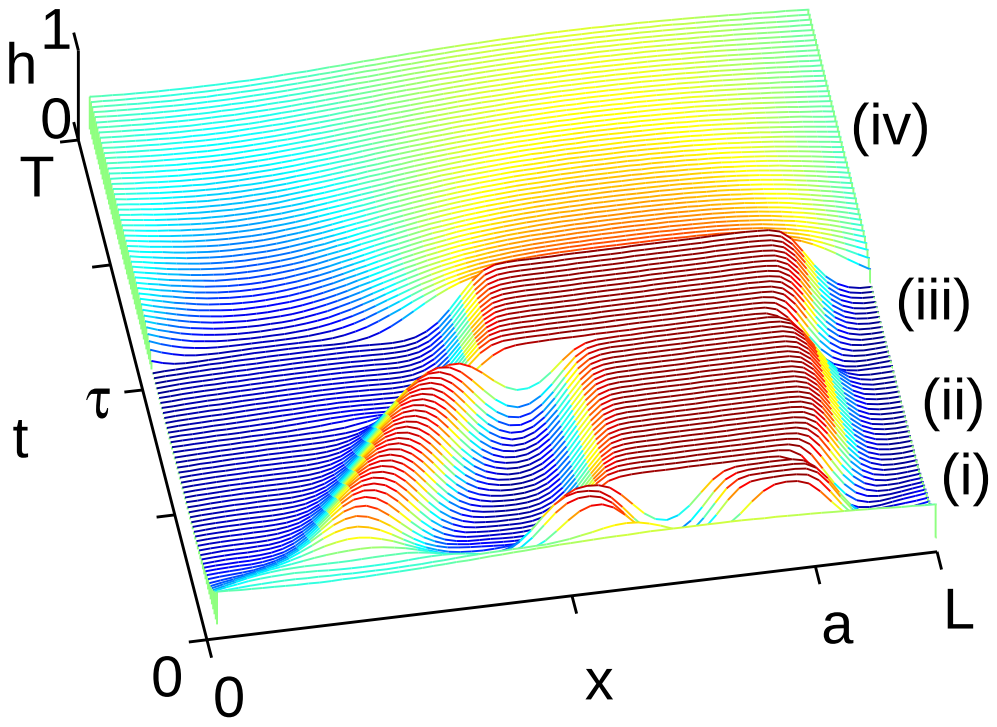

FIG. 2: Space-time plot of one temporal period of the evolution of the film thickness profile for a film of dielectric liquid in a capacitor. Shown is one spatial period. The different phases (i)-(iv) indicated to the right are explained in the main text. Parameters are $\bar{h} = 0.5$, $\psi = 0.5$, $L = 32$, $\phi = 5$, $T = 5000$, $\omega = 1$, $A = 0.001$, $\varepsilon = 2.5$ and $f_{\rm ext} = 0$. The starting time is well after initial transients have decayed.

To obtain a minimal set of parameters we introduce the scales $3\gamma\eta/d\kappa_{el}^2$, $\sqrt{\gamma d/\kappa_{el}}$, and d for t, x, and h, respectively. The electrostatic 'spreading coefficient' is defined by $\kappa_{el} = \varepsilon_0\varepsilon_1 U_0^2/2d^2$. The resulting dimensionless equations correspond to (1)-(5) with $3\eta = \gamma = d = \varepsilon_0\varepsilon_1 U_0^2/2 = 1$. For simplicity we assume $A_u = -A_l$ and obtain the dimensionless Hamaker constant $A = A_l/6\pi d^3\kappa_{el}$. All results are given in terms of dimensionless quantities.

We characterize the ratchet using two measures, the asymmetry ratio $\phi = (L-a)/a$ of the spatial variation $\Phi(x)$ and the flashing ratio $\omega = \tau/(T-\tau)$ of the temporal switching $\Omega(t)$. Zero

net transport is expected for a symmetrical ratchet, i.e. for $\phi = 1$. The resulting transport is quantified by the mean velocity $\bar{v} = \bar{j}/\bar{h}$ where $\bar{j} = (1/TL)\int_0^T dt \int_0^L dx\, j(x,t)$ is the mean flow along the substrate and $j(x,t) = -h^3(\partial_x p - f_{\rm ext})$.

Figure 2 shows a typical example of the film evolution during one ratchet cycle allowing to distinguish four phases. (i) When the ratchet is switched on the film is nearly flat but rapidly evolves a surface instability with a wavelength given approximately by the corresponding spinodal length [20]. (ii) Next, the evolving profile coarsens accelerated by the gradients of the ratchet potential. (iii) In an ideal situation only one drop remains, corresponding to the equilibrium structure on the heterogeneous wettability pattern produced by the ratchet potential [16]. (iv) Finally, after switching off the ratchet the drop starts to spread rapidly under the influence of van der Waals forces until the next cycle starts.

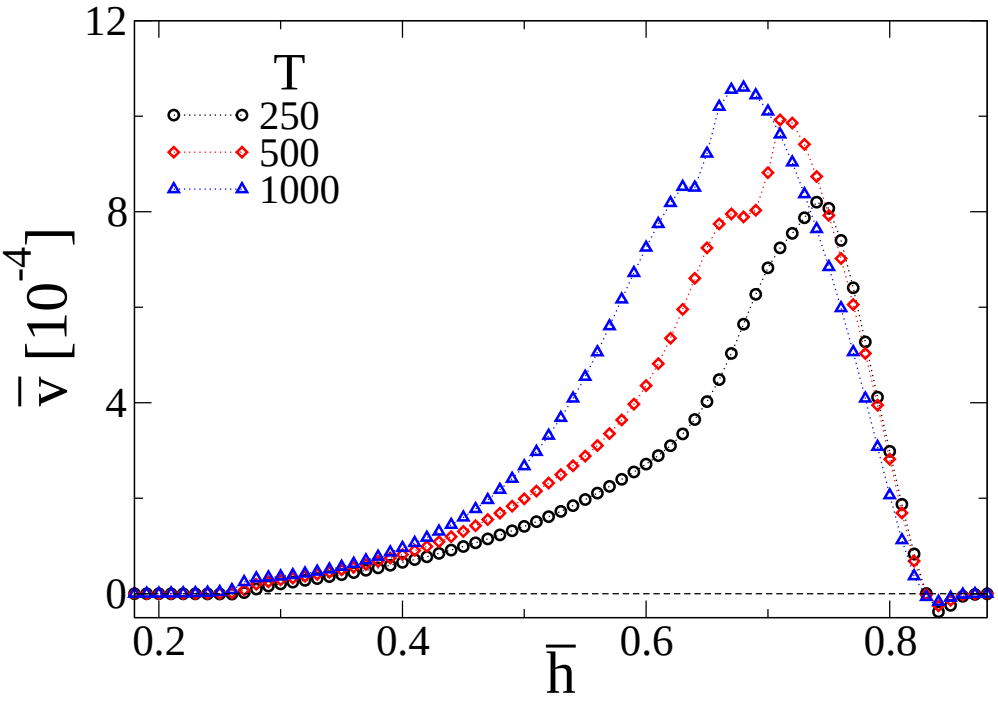

FIG. 3: Dependence of the mean velocity $\bar{v}$ on the liquid level in the capacitor, i.e. on the mean film thickness $\bar{h}$, for various flashing periods T as indicated in the legend. The remaining parameters are as in Fig. 2.

The competing influence of the various parameters allows to tune the transport properties by adjusting the relative importance of the various phases. As shown in Fig. 3 the transport is strongest for intermediate film thicknesses. A film of intermediate thickness in a homogeneous electric field ($\Phi(x) = \Omega(t) = 1$) dewets spinodally with a wavelength well below the used spatial period of the

ratchet. Therefore the ongoing coarsening interacts with the flow induced by the spatial asymmetry and leads to a nontrivial dependence of the mean velocity on the film thickness. For very small or large film thicknesses the stabilizing van der Waals terms are dominating and the mean velocity approaches rapidly zero. Note also the flow reversal, albeit with a small mean velocity, for large $\bar{h} \gtrsim 0.85$. Further calculations (not shown) demonstrate the monotonous increase of the mean velocity with increasing asymmetry ratio ϕ or amplitude ψ of the ratchet potential for otherwise constant parameters.

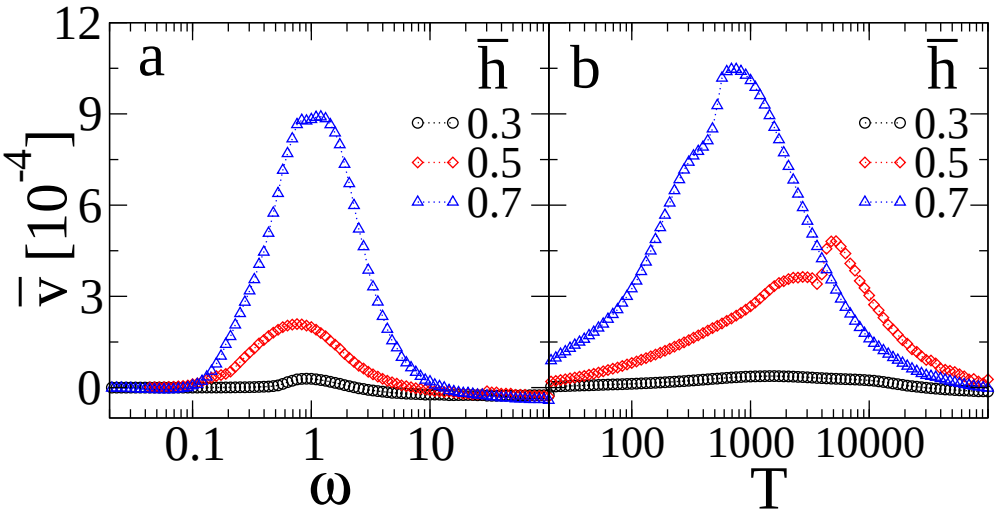

FIG. 4: Variation of the mean velocity $\bar{v}$ in dependence of (a) the flashing ratio ω (for T=500) and (b) the flashing period T (for $\omega = 1$) for various film thicknesses as given in the legends. The remaining parameters are as in Fig. 2.

The flashing characteristics of the ratchet have a very pronounced effect on the transport. Figures 4 (a) and (b) present the non-monotonous dependencies of the flow on the flashing ratio ω and period T, respectively. For small ω the flow is practically zero, since the time for dewetting is too short to trap a considerable amount of liquid at the spots of high wettability. Increasing ω increases the velocity until it reaches a maximum at $\omega \approx 1$. Beyond the maximum the flow decreases again because less and less time remains for the spreading. For large ω one observes a flow reversal.

The dependence of the velocity on the flashing period T is similar but shows around the flow maximum a particularly interesting non-monotonous behavior that is due to coarsening. For small periods the fluid has neither enough time to dewet nor to spread and the resulting mean transport is small. For large periods both processes reach the respective equilibrium structure well before the next switching, i.e. most time is spend waiting and the mean velocity decreases approximately

as $1/T$.

Assuming an ideal combination of ratchet properties and intrinsic length and time scales, and approximating the intermediate drops at the field maxima as point-like objects, all the liquid moves by $a - L/2$ in one cycle of length T. For a film of mean thickness $\bar{h}$ this yields a mean flow of $\bar{j}_{ideal} = \bar{h}(a - L/2)/T$, i.e. the mean velocity is $\bar{v}_{ideal} = (a - L/2)/T$. The maximal spatial asymmetry is given by $a = L$, i.e. $\bar{j}_{max} = \bar{h}L/2T$ and $\bar{v}_{max} = L/2T$. In a real system, however, several effects keep the mean velocity below the ideal value. For optimal parameters in simulations we reach about 30% of $\bar{v}_{ideal}$ (Fig. 4 (b) for $\bar{h} = 0.7$ and $T \approx 10000$).

For practical applications transport against an external force is of crucial importance. In the reference system of a uniform substrate no work is performed and all energy is lost via viscous dissipation. This is not the case for a thin film ratchet under load, i.e. $f_{\rm ext} \neq 0$ in (1). Switching off the ratchet, $f_{\rm ext} < 0$ induces a negative macroscopic flow. Simple mechanical realizations of $f_{\rm ext}$ are an inclined substrate or centrifugal forces yielding a constant $f_{\rm ext}$ independent of the film thickness. The flashing ratchet generates a positive flow, i.e. mechanical work is performed against the external force. The transport under load is characterized by the (mechanical) energy transport efficiency

$$\nu_{\rm eff} = -\frac{\dot{W}}{\dot{Q}} \tag{6}$$

where

$$\dot{W} = \frac{1}{TL}\int_0^L dx \int_0^T dt\, j\, f_{\rm ext} \tag{7}$$

denotes the mechanical work performed per unit time and

$$\dot{Q} = -\frac{1}{TL}\int_0^L dx \int_0^T dt\, j\, \partial_x p \tag{8}$$

denotes the interaction energy consumed per time. The mean velocity and transport efficiency are shown in Figs. 5 (a) and (b). The transport efficiency behaves non-monotonically. It increases for small loads, reaches a maximum and decreases for higher loads. It becomes negative when the flow reverses. Then the ratchet can no longer perform work against the external force.

Finally, we discuss the feasibility of a fluid ratchet employing spatially inhomogeneous electric fields by estimating the acting forces and relevant time and length scales for millimetric, microscopic and nanoscopic fluidic systems. Typical material constants for thin films in capacitors are taken from [23, 24, 25] and references therein. Applying a voltage of 100 V over a gap of 2 mm width, a 1 mm film of silicon oil feels an electrostatic pressure of $p_{el} \approx 0.1 \mathrm{N\,m^{-2}}$ corresponding

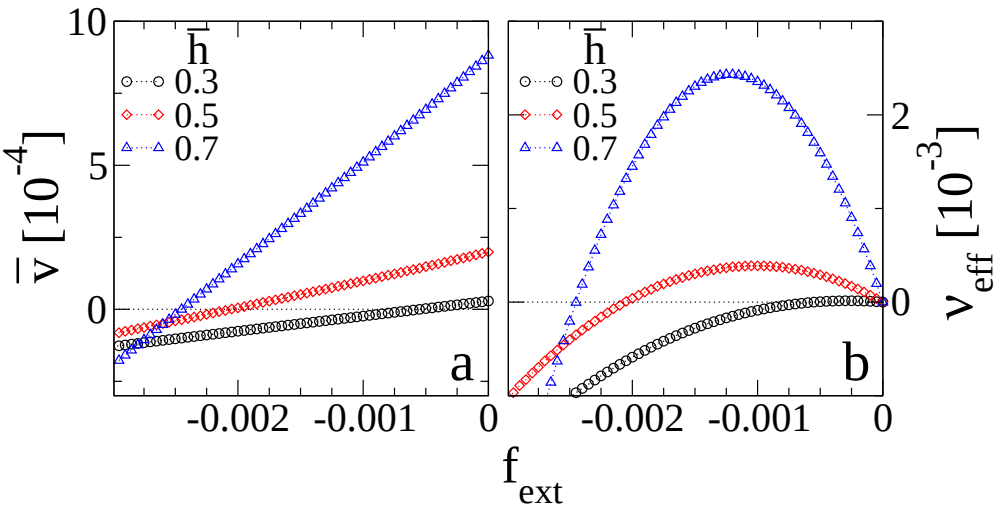

FIG. 5: The influence of an external load $f_{\rm ext}$. Shown are the variations of (a) the mean velocity $\bar{v}$ and (b) the transport efficiency $\nu_{\rm eff}$ with $f_{\rm ext}$ for various mean film thicknesses $\bar{h}$ as indicated in the legends. The remaining parameters are as in Fig. 2 except for $T = 500$.

approximately to the curvature pressure in a drop of 1 mm height with $\theta_0 = 10\,^\circ$ equilibrium contact angle. Thinner films can be influenced by a lower voltage [12]. For instance, for a 10 μm oil film in a 20 μm gap for $U_0 = 10\,$V we find $p_{el} \approx 10\,{\rm N\,m^{-2}}$, equivalent to the curvature pressure in a droplet of 10 μm height and $\theta_0 = 10\,^\circ$. In principle, nanofluidic transport of polymer melts is also feasible. For a 30 nm film of liquid polystyrene in a 100 nm gap which is electrostatically patterned ($U_0 = 10\,$V) [25], $p_{el} \approx 10^4$N/m^2 equivalent to the curvature pressure for a droplet of 30 nm height and 300 nm width. Note, however, that for ultrathin films the disjoining pressure is of the same order of magnitude [22].

Beside the length scales also the time scales are of uttermost importance. The scale $\tau = 3\gamma\eta/d\kappa_{el}^2$ reflects the relevant properties responsible for the relaxation towards the flat film. For a 5cS silicon oil the estimate gives a timescale of 10 to 10^3 s, i.e. the viscous flow is rather slow. Using, however, water films of thicknesses between 10 μm ($U_0 = 10$V) and 1 mm ($U_0 = 100$V) the time scale ranges from 10^{-5} to 10^{-3} s resulting in fast transport.

In conclusion, we have shown that a flashing ratchet produces a macroscopic transport in a liquid film with a free surface on a feasible time scale. There exist regimes of maximum transport selected by the spatial and temporal properties of the ratchet, which depend on the characteristics of the thin film. For a spatial period of the ratchet which is considerably larger than the length scale of the spinodal instability of the flat film subjected to a homogeneous potential the coarsening

dynamics influences the transport in a non-trivial way.

This work was supported by the EU under grant MRTN-CT-2004-005728. K. J. was supported by grants from the CNES and the Humboldt-Foundation.

---

[1] R. D. Astumian, Science **276**, 917 (1997).

[2] R. D. Astumian and P. Hänggi, Phys. Today **55**, 33 (2002).

[3] P. Hänggi, F. Marchesoni, and F. Nori, Ann. Phys.-Berlin **14**, 51 (2005).

[4] J. Rousselet, L. Salome, A. Ajdari, and J. Prost, Nature **370**, 446 (1994).

[5] S. Matthias and F. Müller, Nature **424**, 53 (2003).

[6] F. Jülicher, A. Ajdari, and J. Prost, Rev. Mod. Phys. **69**, 1269 (1997).

[7] P. Curie, J. Physique (Paris) **III**, 393 (1894).

[8] A. D. Stroock, R. F. Ismagilov, H. A. Stone, and G. M. Whitesides, Langmuir **19**, 4358 (2003).

[9] D. Quéré and A. Ajdari, Nat. Mater. **5**, 429 (2006).

[10] H. Linke, B. J. Alemán, L. D. Melling, M. J. Taormina, M. J. Francis, C. C. Dow-Hygelund, V. Narayanan, R. P. Taylor, and A. Stout, Phys. Rev. Lett. **96**, 154502 (2006).

[11] A. Buguin, L. Talini, and P. Silberzan, Appl. Phys. A-Mater. Sci. Process. **75**, 207 (2002).

[12] Z. Lin, T. Kerle, S. M. Baker, D. A. Hoagland, E. Schäffer, U. Steiner, and T. P. Russell, J. Chem. Phys. **114**, 2377 (2001).

[13] E. Schäffer, T. Thurn-Albrecht, T. P. Russell, and U. Steiner, Europhys. Lett. **53**, 518 (2001).

[14] M. D. Morariu, N. E. Voicu, E. Schäffer, Z. Lin, T. P. Russell, and U. Steiner, Nat. Mater. **2**, 48 (2003).

[15] K. Kargupta and A. Sharma, Phys. Rev. Lett. **86**, 4536 (2001).

[16] U. Thiele, L. Brusch, M. Bestehorn, and M. Bär, Eur. Phys. J. E **11**, 255 (2003).

[17] A. Sidorenko, S. Minko, K. Schenk-Meuser, H. Duschner, and M. Stamm, Langmuir **15**, 8349 (1999).

[18] U. Thiele and E. Knobloch, Physica D **190**, 213 (2004).

[19] M. Bestehorn, A. Pototsky, and U. Thiele, Eur. Phys. J. B **33**, 457 (2003).

[20] A. Oron, S. H. Davis, and S. G. Bankoff, Rev. Mod. Phys. **69**, 931 (1997).

[21] P.-G. de Gennes, Rev. Mod. Phys. **57**, 827 (1985).

[22] J. N. Israelachvili, *Intermolecular and Surface Forces* (Academic Press, London, 1992).

[23] D. Merkt, A. Pototsky, M. Bestehorn, and U. Thiele, Phys. Fluids **17**, 064104 (2005).

[24] A. Engel and J. B. Swift, Phys. Rev. E **62**, 6540 (2000).

[25] Z. Lin, T. Kerle, T. P. Russell, E. Schäffer, and U. Steiner, Macromolecules **35**, 3971 (2002).